A New Read Channel Model for Patterned Media Storage

Seyhan Karakulak, Paul H. Siegel, *Fellow, IEEE*, Jack K. Wolf, *Life Fellow, IEEE*, and H. Neal Bertram, *Life Fellow, IEEE*

Center for Magnetic Recording Research, University of California at San Diego, La Jolla, CA 92093-0401 USA

It is conceivable that early generations of patterned media will utilize read heads whose dimensions are several times larger than an "island" of magnetization. For such a scenario, we propose a "multiple islands per read head" model where the output from the read head is a function of the magnetization from several independently written tracks of islands. In particular, we focus on a "3 islands per read head" model where the output from the read head is a function of the magnetization from three independently written tracks of islands. The readback signal is determined from a finite track-width magnetoresistive (MR) head model using reciprocity calculations, and two noise sources—island position jitter and AWGN electronics noise—are considered. By sampling the noisy signal at intervals corresponding to the down-track island separation, we obtain a discrete-time readback channel model whose performance is obtained under maximum-likelihood sequence detection.

***Index Terms*—Island position jitter, "multiple islands per read head", patterned media.**

I. Introduction

In current film media, the increase in areal density has been achieved primarily by scaling grain diameters and the number of magnetic grains per recorded bit. A sufficient number of grains per bit is necessary to maintain an acceptable signal-to-noise ratio (SNR). However, as grain sizes are reduced, thermal fluctuations can reverse spontaneously the grain magnetization direction.

Patterned media where magnetic bits are recorded on predefined, single domain "islands" may provide an alternative to conventional continuous media. For this new type of media, not only will the media manufacturing process change, but also the head design, signal processing, and many other system features will be affected [2]–[4].

It is conceivable that early generations of patterned media will utilize read heads whose dimensions are several times larger than an island of magnetization. For such a scenario, we propose a "multiple islands per read head" model where the output from the read head is a function of the magnetization from several independently written tracks of islands.

The readback signal is determined from a finite track-width magnetoresistive (MR) head model using reciprocity calculations [1]. Two noise sources—island position jitter and AWGN electronics noise—are considered. By sampling the noisy signal at intervals corresponding to the down-track island separation, we obtain a discrete-time readback channel model whose performance in AWGN is obtained.

The paper is organized as follows. In Section II, we introduce the "multiple islands per read head" model. In particular, we focus on a "3 islands per read head" model. We continue to Section III, in which we introduce AWGN electronics noise into our models. In the absence of inter-symbol interference (ISI), we estimate the performances of the "3 islands per read head" model and a single track model. For the ISI case, we compute the performances of the "3 islands per read head" model and a single track model using maximum-likelihood sequence detection. In Section IV, we introduce an island jitter noise model. We show that this noise source is non-Gaussian.

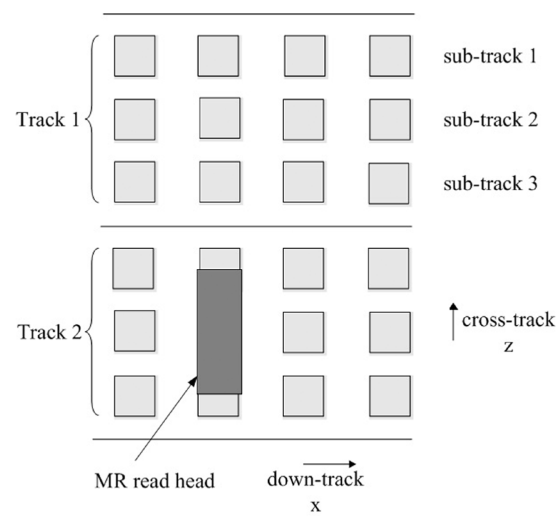

Fig. 1. "3 islands per read head."

II. "Multiple Islands per Read Head" Model

In our "multiple islands per read head" model, the magnetized islands are assumed to be configured in a square grid with each island representing a single bit. A track consists of multiple parallel sub-tracks, and the read head, when centered over the middle sub-track, spans a specified fraction of the outer sub-tracks, as shown schematically in Fig. 1 for a track with three parallel sub-tracks.

The islands are arranged in a square array with dimension s and with a film thickness h. A center-to-center island spacing B is equal to $2s$ (Fig. 2). Each cross-track triplet of islands represents a recorded "symbol."

Reading is accomplished with a finite track-width shielded magnetoresistive (MR) head with infinitely wide shields. The top view of such a shielded MR head is shown in Fig. 3. In the figure, W stands for the head width, t stands for the thickness of the MR element, and g stands for the gap from shield to the MR element.

Digital Object Identifier 10.1109/TMAG.2007.912837

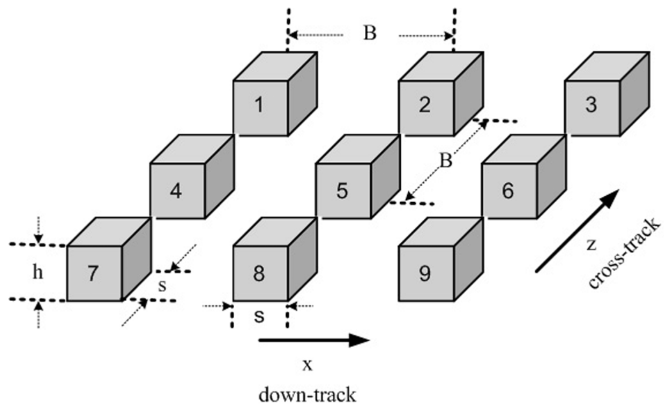

Fig. 2. Configuration of the patterned islands.

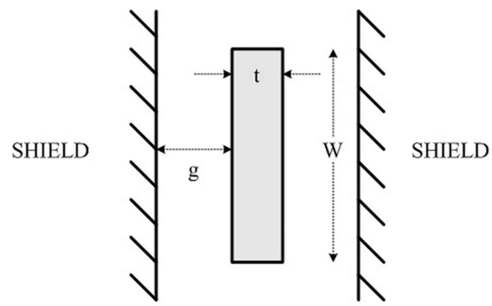

Fig. 3. Top view of a shielded MR head.

In the absence of a soft underlayer (SUL), the head potential distribution $\Psi(\mathrm{x,y,z})$ is obtained using reciprocity calculations [1]

$$\begin{aligned}\Psi(\mathrm{x,y,z}) &= \Bigg(\left\{ \frac{\mathrm{y}}{4\pi \mathrm{g}} \log\left[\frac{R+(z-z')}{R-(z-z')}\right] + \frac{\mathrm{g}+\frac{\mathrm{t}}{2}+x}{2\pi g} \right. \\ &\qquad \left. .\tan^{-1}\left[\frac{(z-z')(x-x')}{yR}\right]\right\}\Bigg|_{x'=-g-t/2}^{-t/2} \\ &\quad + \frac{1}{2\pi}\tan^{-1}\left[\frac{(z-z')(x-x')}{yR}\right]\Bigg|_{x'=-t/2}^{t/2} \\ &\quad + \left\{-\frac{y}{4\pi g}\log\left[\frac{R+(z-z')}{R-(z-z')}\right] + \frac{g+\frac{t}{2}-x}{2\pi g}\right. \\ &\qquad \left. .\tan^{-1}\left[\frac{(z-z')(x-x')}{yR}\right]\right\}\Bigg|_{x'=t/2}^{t/2+g}\Bigg)\Bigg|_{z'=-W/2}^{W/2}\end{aligned} \tag{1}$$

where $R=\sqrt{(x-x')^2+y^2+(z-z')^2}$.

The surface plot of the head potential at $y = 5$ nm is shown in Fig. 4.

The readback signal produced by the head centered at (0,0) from an island centered at (x_0, z_0) is the integral of the head potential distribution over that island

$$V(x_0,z_0) = \int_{x_0-s/2}^{x_0+s/2}\int_{z_0-s/2}^{z_0+s/2} (\Psi(x,d,z)-\Psi(x,d+h,z))\,dxdz. \tag{2}$$

In (2), d is the flying height.

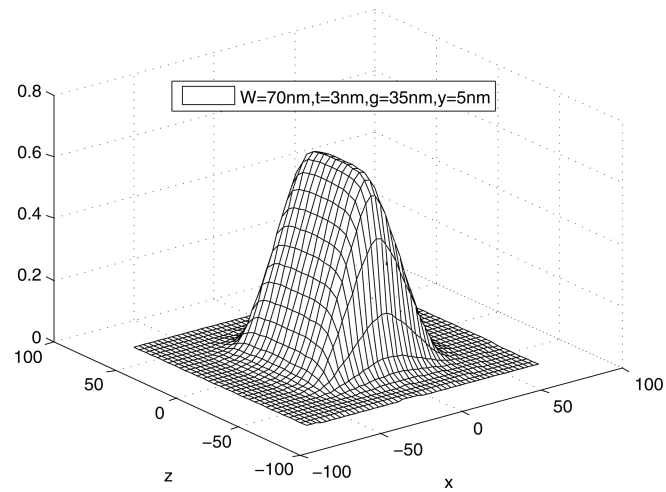

Fig. 4. Surface plot of the head potential distribution versus down-track and cross-track distance for a shielded MR head with infinitely wide shields.

For a given thickness of the SUL ℓ in the y direction, choose the smallest positive integer N such that for a given ε

$$|\Psi(x, 2(\mathrm{N}+1)\ell + y, z) - \Psi(x, 2(\mathrm{N}+1)\ell - y, z)| < \varepsilon. \tag{3}$$

In the presence of the SUL, the head potential distribution is computed using the multiple images calculation

$$\begin{aligned}\Psi_{\mathrm{SUL}}(x,y,z) = \sum_{i=1}^{N} (\Psi(x, 2i\ell + y, z) \\ -\Psi(x, 2i\ell - y, z)) + \Psi(x,y,z).\end{aligned} \tag{4}$$

The readback signal from the island centered at (x_0, z_0) is then given by

$$\begin{aligned}V_{\mathrm{SUL}}(x_0,z_0) = \int_{x_0-s/2}^{x_0+s/2}\int_{z_0-s/2}^{z_0+s/2} (\Psi_{\mathrm{SUL}}(x,d,z) \\ -\Psi_{\mathrm{SUL}}(x,d+h,z))\,dxdz.\end{aligned} \tag{5}$$

We can control the inter-island interference in the cross-track direction by varying W and in the down-track direction by varying g. When the head senses signals from m and n islands in the cross-track and down-track directions, respectively, the discrete-time readback model can be represented by an $m \times n$ channel response matrix

$$H = [\underline{h}_1, \underline{h}_2, \ldots, \underline{h}_{\mathrm{n}}]. \tag{6}$$

Here, each $\underline{h}_{\mathrm{i}}$ is an m-tuple of real numbers. Each entry of H represents the relative contribution of islands the head senses.

Denote a symbol $\underline{u}$ by an m-tuple. The discrete-time readback model then takes the form of a one-dimensional linear channel with symbols $\underline{u}_{\mathrm{i}}$ as inputs and a scalar v_i as the output, with input–output relationship determined by the channel response matrix, as depicted for $n = 3$ in Fig. 5.

From now on, we will focus on a channel response matrix where $m = 3$ and $n = 3$ which reflects ISI. The assumed

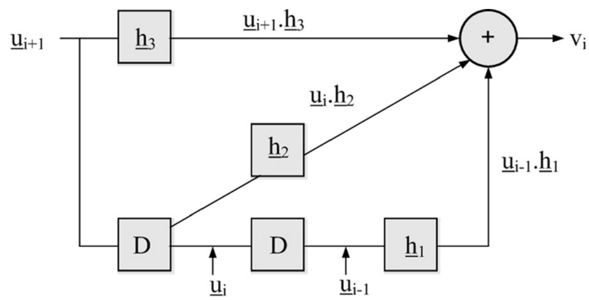

Fig. 5. Read head channel model.

TABLE I
SYMBOLS AND SYMBOL VARIANTS

0	1'	1''	1'''	2'	2''	2'''	3
−	+	−	−	+	+	−	+
−	−	+	−	+	−	+	+
−	−	−	+	−	+	+	+

symmetries of the head-medium geometries yield a channel response matrix of the form

$$H = \begin{pmatrix} r & p & r \\ t & q & t \\ r & p & r \end{pmatrix}. \tag{7}$$

If an arbitrary pattern of magnetization can be written on the 3 islands, there will be eight possible recorded symbols as shown in Table I. The alphabet that includes eight possible symbols is denoted by U, where $U = \{0, 1', 1'', 1''', 2', 2'', 2''', 3\}$. However, symmetries of the channel response matrix can reduce the number of distinguishable symbols. The integer that is used to label a symbol corresponds to the number of $+$ coded bits of the symbol. In order to distinguish the symbols with the same integer, we use primes.

We define three different head response matrices of the form

$$H_I = \begin{pmatrix} 0 & 0 & 0 \\ \beta & b & \beta \\ 0 & 0 & 0 \end{pmatrix} H_{II} = \begin{pmatrix} \beta & b & \beta \\ \beta & b & \beta \\ \beta & b & \beta \end{pmatrix} H_{III} = \begin{pmatrix} \alpha & a & \alpha \\ \beta & b & \beta \\ \alpha & a & \alpha \end{pmatrix}.$$

In the above matrices, the constants b, β, a, α, where $b \neq \beta$ and $a \neq \alpha$, represent the relative contribution of readback signals the head produces from the islands it senses. The matrix H_I represents a single track model where the read head width is slightly larger than the island size. In H_{II}, the head spans all three islands, and in H_{III}, the head partially spans the outer sub-tracks.

When the head response matrix is H_{II}, the head can not distinguish the variants of the symbols 1 and 2. To show that, let us define the symbols $\underline{u}_{i-1}$, $\underline{u}_i$, and $\underline{u}_{i+1}$ as shown in Table II where $\{u_{i-1,1}, u_{i-1,2}, u_{i-1,3}, \ldots, u_{i+1,1}, u_{i+1,2}, u_{i+1,3}\}$ are coded bits. When the previous, current, and next symbols are $\underline{u}_{i-1}$, $\underline{u}_i$, and $\underline{u}_{i+1}$, respectively, the readback signal equals

$$v_{II} = b(u_{i,1} + u_{i,2} + u_{i,3}) + \beta(u_{i-1,1} + u_{i-1,2} + u_{i-1,3} + u_{i+1,1} + u_{i+1,2} + u_{i+1,3}). \tag{8}$$

From the readback signal, it is seen that we can not distinguish the variants of 1 and 2, since those variants include the same number of $+$ and $-$ coded bits. Therefore, for the head response matrix H_{II}, the number of distinguishable symbols is four and this corresponds to an information rate of 2/3 bits per island. We select 4 symbols out of 8 symbols for the code alphabet of H_{II}. For example, we could use the code alphabet $U_{II} = \{0, 1', 2', 3\}$.

TABLE II
PREVIOUS, CURRENT, AND NEXT SYMBOLS

$\underline{u}_{i-1}$	$\underline{u}_i$	$\underline{u}_{i+1}$
$u_{i-1,1}$	$u_{i,1}$	$u_{i+1,1}$
$u_{i-1,2}$	$u_{i,2}$	$u_{i+1,2}$
$u_{i-1,3}$	$u_{i,3}$	$u_{i+1,3}$

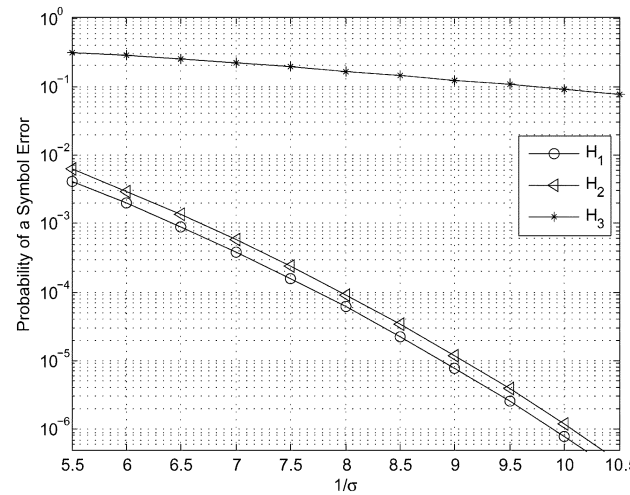

Fig. 6. Probability of a symbol error for H_1, H_2, and H_3 versus $1/\sigma$.

In a similar way, the readback signal for the head response matrix H_{III} is

$$v_{III} = a(u_{i,1} + u_{i,3}) + bu_{i,2} + \beta(u_{i-1,2} + u_{i+1,2}) + \alpha(u_{i-1,1} + u_{i-1,3} + u_{i+1,1} + u_{i+1,3}). \tag{9}$$

It is seen that when we interchange $u_{i-1,1}$ and $u_{i-1,3}$, $u_{i,1}$ and $u_{i,3}$, $u_{i+1,1}$ and $u_{i+1,3}$, the readback signal does not change. If those two coded bits are different, swapping these bits is equal to changing the symbol $1'$ to $1'''$, $2'$ to $2'''$ or vice versa. Therefore, the read head is not able to distinguish the symbols $1'$ and $1'''$, $2'$ and $2'''$ from each other. In this case, the number of distinguishable symbols is six corresponding a rate $\log_2(6)/3 \approx 0.8617$ bits per island. We select 6 symbols out of 8 symbols for the code alphabet of H_{III}. For example, we could use the code alphabet $U_{III} = \{0, 1', 1'', 2', 2'', 3\}$.

In our channel model, we consider two noise sources: AWGN electronics noise and medium noise. The replay transducer and the readback circuitry generate the stationary electronics noise. This noise source is modeled as bandwidth- limited AWGN. We assume that AWGN is a Gaussian with mean zero and variance σ^2. The dominant component of the medium noise arises from the randomness of the island locations. This nonstationary component is referred to as "jitter noise."

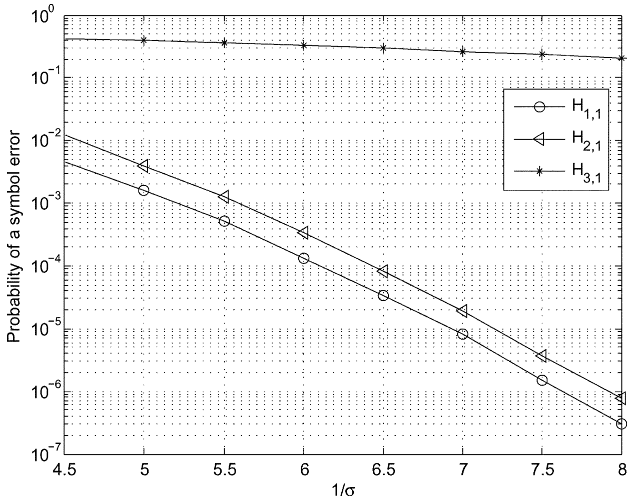

Fig. 7. Probability of a symbol error for $H_{1,1}$, $H_{2,1}$, and $H_{3,1}$ versus $1/\sigma$.

III. Performance Analysis in AWGN

When no ISI occurs and the noise is AWGN, we can compute the exact probability of a symbol error in terms of Q-functions by the approach used for a pulse amplitude modulation (PAM) communication system. Assume that there are M distinct readback voltages the head produces. We denote them with a_i where $i \in \{1,2,\ldots,M\}$ and $a_j > a_k$ for any $j > k$. When all the readback voltages occur with equal probability, the probability of a symbol error is

$$P_{\mathrm{sym}} = \frac{1}{M}\left\{Q\left(\frac{a_2-a_1}{2\sigma}\right)+Q\left(\frac{a_M-a_{M-1}}{2\sigma}\right) + \sum_{i=2}^{M-1}\left[Q\left(\frac{a_i-a_{i-1}}{2\sigma}\right)+Q\left(\frac{a_{i+1}-a_i}{2\sigma}\right)\right]\right\}. \quad (10)$$

When a head has a small gap g, no ISI occurs. Here, $n=1$, but we can still use a 3×3 head response matrix. We consider the following responses:

$$H_1 = \begin{pmatrix} 0 & 0 & 0 \\ 0 & 0.48 & 0 \\ 0 & 0 & 0 \end{pmatrix} H_2 = \begin{pmatrix} 0 & 0.48 & 0 \\ 0 & 0.48 & 0 \\ 0 & 0.48 & 0 \end{pmatrix}$$
$$H_3 = \begin{pmatrix} 0 & 0.16 & 0 \\ 0 & 0.48 & 0 \\ 0 & 0.16 & 0 \end{pmatrix}.$$

We define $V_{\max}$ as the maximum voltage level the read head produces. Here, we have $V_{\max}^{(1)} = 0.48$, $V_{\max}^{(2)} = 1.44$, and $V_{\max}^{(3)} = 0.80$.

For H_1, H_2, and H_3, when all the code symbols are recorded with equal probability, the formula (10) reduces to

$$P_{\mathrm{sym}}^{(1)} = Q\left(\frac{V_{\max}^{(1)}}{\sigma^{(1)}}\right) = Q\left(\frac{0.48}{\sigma^{(1)}}\right) \quad (11)$$

$$P_{\mathrm{sym}}^{(2)} = \frac{3}{2}Q\left(\frac{V_{\max}^{(2)}}{3\sigma^{(2)}}\right) = \frac{3}{2}Q\left(\frac{1.44}{3\sigma^{(2)}}\right) \quad (12)$$

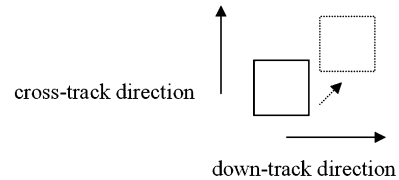

Fig. 8. A shifted island in the down-track and cross-track directions.

$$P_{\mathrm{sym}}^{(3)} = \frac{5}{3}Q\left(\frac{V_{\max}^{(3)}}{5\sigma^{(3)}}\right) = \frac{5}{3}Q\left(\frac{0.80}{5\sigma^{(3)}}\right). \quad (13)$$

In Fig. 6, the probability of a symbol error for the head responses H_1, H_2, and H_3 versus $1/\sigma$ is shown.

We next introduce ISI by increasing the gap g. We set the value of the gap g so that the left and the right neighboring symbols contribute 1/3 as much as the center symbol. For detection, in the presence of AWGN, we will use a maximum-likelihood sequence detector matched to the head response matrices

$$H_{1,1} = \begin{pmatrix} 0 & 0 & 0 \\ 0.20 & 0.60 & .20 \\ 0 & 0 & 0 \end{pmatrix} H_{2,1} = \begin{pmatrix} 0.20 & 0.60 & 0.20 \\ 0.20 & 0.60 & 0.60 \\ 0.20 & 0.20 & 0.20 \end{pmatrix}$$
$$H_{3,1} = \begin{pmatrix} 0.0\overline{6} & 0.20 & 0.0\overline{6} \\ 0.20 & 0.60 & 0.20 \\ 0.0\overline{6} & 0.20 & 0.0\overline{6} \end{pmatrix}.$$

The probability of a symbol error for $H_{1,1}$, $H_{2,1}$, and $H_{3,1}$ versus $1/\sigma$ is obtained by simulations and is shown in Fig. 7.

IV. Island Jitter Noise Model

Let us assume that an island can be shifted from its ideal location in both the down-track and cross-track directions as shown in Fig. 8.

We model these shifts as independent, zero-mean Gaussian random variables δx and δz, with variances $\sigma_{\delta x}^2$ and $\sigma_{\delta z}^2$, respectively. The readback voltage induced in a head centered at (0,0) by an island centered at $(x+\delta x, z+\delta z)$ is expressed using a Taylor series expansion

$$\begin{aligned} V(x+\delta x, z+\delta z) =& V(x,z) + \delta x V_x(x,z) + \delta z V_z(x,z) \\ &+ \frac{1}{2}\left[(\delta x)^2 V_{xx}(x,z) + 2\delta x \delta z V_{xz}(x,z) \right. \\ &\left. + (\delta z)^2 V_{zz}(x,z)\right] + \xi(x,z) \\ =& V(x,z) + e(x,z) + \xi(x,z) \end{aligned} \quad (14)$$

where $\xi(x,z)$ is the modeling error due to approximating the shifted readback voltage with the first- and second-order derivative terms. The second-order approximation to the island jitter is $e(x,z)$, which is defined as

$$\begin{aligned} e(x,z) =& V(x,z) + \delta x V_x(x,z) + \delta z V_z(x,z) \\ &+ \frac{1}{2}\left[(\delta x)^2 V_{xx}(x,z) + 2\delta x \delta z V_{xz}(x,z) \right. \\ &\left. + (\delta z)^2 V_{zz}(x,z)\right]. \end{aligned} \quad (15)$$

For the head response matrix H_2, define

$$V \doteq V(0+\delta x, 0+\delta z) - V(0,0) \quad (16)$$

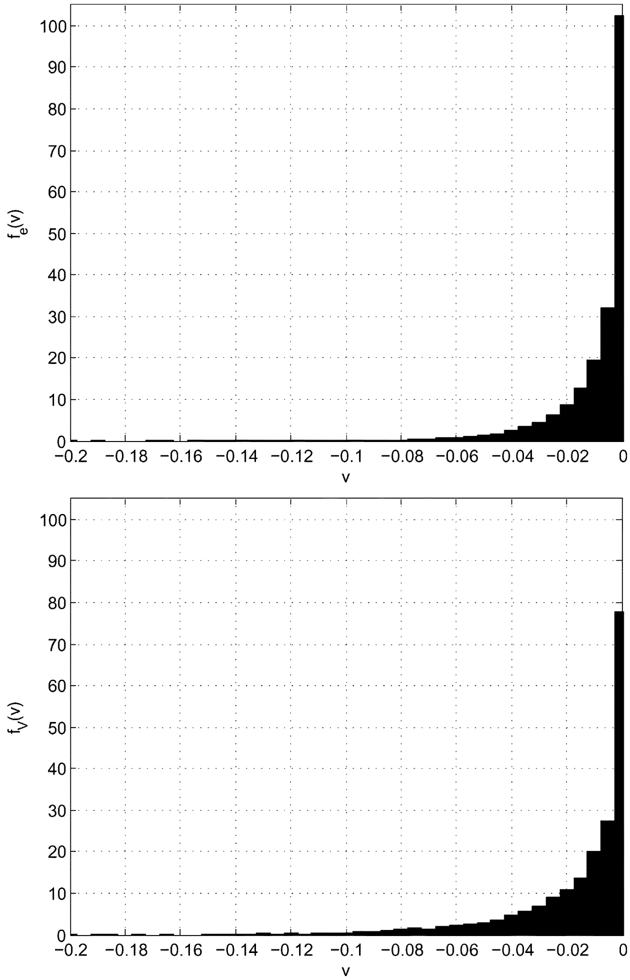

Fig. 9. Probability density function for V and e.

and

$$e \doteq e(0,0) \tag{17}$$

where V represents the jitter-induced readback voltage and e represents the second order approximation to the jitter-induced readback voltage. The normalized histograms, which are $f_V(v)$ and $f_e(v)$ for V and e, respectively, are obtained by simulations and shown in Fig. 9. It is seen that V is non-Gaussian. The second approximation to the island jitter can capture this property, whereas the first-order approximation to the island jitter is Gaussian. Obtaining the histogram of the jitter noise from (17) is computationally intensive. A much simpler method for obtaining this histogram results from the second-order approximation given in (16).

Assume that the island jitter is independent from island to island. In the non-ISI case, for $m = 3$, the total jitter noise is the sum of contributions from the top, center, and bottom island

$$e_{\text{total}} = e(0,B) + e(0,0) + e(0,-B). \tag{18}$$

This noise source is symbol dependent and non-Gaussian.

V. Conclusion

In this work, we introduced a "multiple islands per read head" model for patterned media recording. We computed the readback signal from a finite track-width MR head model using reciprocity calculations. We considered two noise sources—island position jitter and electronics noise. We introduced a vector-input, scalar-output discrete model for the readback channel. We determined the performance of this channel in AWGN with and without ISI using maximum-likelihood sequence detection. We showed that the jitter noise is symbol dependent and non-Gaussian.

Acknowledgment

This work was supported by the Patterned Media Project at the Center for Magnetic Recording Research, University of California, San Diego.

References

[1] S. W. Yuan and H. N. Bertram, "Off-track spacing loss of shielded MR heads," *IEEE Trans. Magn.*, vol. 30, no. 3, pp. 1267–1273, May 1994.

[2] P. W. Nutter, I. T. Ntokas, and B. K. Middleton, "An investigation of the effects of media characteristics on read channel performance for patterned media storage," *IEEE Trans. Magn.*, vol. 41, no. 11, pp. 4327–4334, Nov. 2005.

[3] P. W. Nutter, I. T. Ntokas, B. K. Middleton, and D. T. Wilton, "Effect of island distribution on error rate performance in patterned media," *IEEE Trans. Magn.*, vol. 41, no. 10, pp. 3214–3216, Oct. 2005.

[4] H. J. Richter, A. Y. Dobin, O. Heinonen, K. Z. Gao, R. J. M. van de Veerdonk, R. T. Lynch, J. Xue, D. Weller, P. Asselin, M. F. Erden, and R. M. Brockie, "Recording on bit-patterned media at densities of 1 Tb/in^2 and beyond," *IEEE Trans. Magn.*, vol. 42, no. 10, pp. 2255–2260, Oct. 2006.

Manuscript received May 31, 2007. Corresponding author: S. Karakulak (e-mail: skarakul@ucsd.edu).